

Received 3 August 2023, accepted 20 August 2023, date of publication 31 August 2023, date of current version 7 September 2023.

Digital Object Identifier 10.1109/ACCESS.2023.3310934

RESEARCH ARTICLE

Quasi-Elliptic Higher-Order Tunable Bandpass Filter With Constant Absolute Bandwidth Using Synchronously Tuned Dual-Mode Resonators

GIRDHARI CHAUDHARY¹, (Member, IEEE),
AND YONGCHAE JEONG², (Senior Member, IEEE)

¹JIANT-IT Human Resource Development Center, Division of Electronics Engineering, Jeonbuk National University, Jeonju-si 54896, South Korea

²Division of Electronics Engineering, Jeonbuk National University, Jeonju-si 54896, South Korea

Corresponding author: Yongchae Jeong (ycjeong@jbnu.ac.kr)

This work was supported in part by the National Research Foundation of Korea (NRF) Grant funded by the Korean Government through the Ministry of Science and ICT (MSIT) under Grant RS-2023-00209081, and in part by the Basic Science Research Program through NRF Grant funded by the Ministry of Education under Grant 2019R1A6A1A09031717.

ABSTRACT Designing a higher-order tunable bandpass filter (BPF) with constant absolute bandwidth (ABW) and identical passband response at every passband frequency tuning state is considered a challenge. In this paper, we propose quasi-elliptic higher-order tunable BPFs that use synchronously tuned dual-mode resonators, which can achieve identical passband frequency response and constant ABW. To achieve identical passband frequency response and constant ABW, all frequency-dependent coupling coefficient and external quality factor are physically realized using series capacitor and shunt varactor. To achieve quasi-elliptic response, transmission zeros are generated at lower and upper sides of passband through cross-coupling between dual-mode resonators. For experimental validation, a prototype of 4th and 6th-order BPFs are designed and fabricated. Experimental results reveal that the passband center frequency of the 4th-order tunable BPF can be tuned from 1.35 to 1.75 GHz (25.82%) with identical passband return loss (RL) of 20 dB and 1-dB constant ABW of 92 ± 1.3 MHz. Similarly, the passband center frequency of 6th-order BPF can be tuned from 1.38 to 1.77 GHz (27.76%) with an identical passband RL of 20 dB and 1-dB constant ABW of 98 ± 1.5 MHz.

INDEX TERMS Dual-mode resonators, identical passband response, tunable bandpass filters.

I. INTRODUCTION

Tunable bandpass filters (BPFs) with identical passband frequency response and constant absolute bandwidth (ABW) are very attractive for better utilization of the frequency spectrum in the next generation communication systems [1]. In recent years, tunable BPFs based on multi-mode resonators have attracted a lot of attention as they have the potential to reduce circuit size [2]. Several tunable BPFs based on dual-mode resonator are presented in the literature including center frequency and bandwidth tunability [3], [4], [5]. In [6] and [7], tunable BPFs based on a synchronously tuned dual-mode resonator are designed and

fabricated. A wideband tunable BPF based on a tunable external Q -factor and the multi-mode resonators is presented in [8]. However, the majority of previously reported tunable BPFs focus on low-order (such as 2nd and 3rd-order) BPF designs [9], [10], [11], [12], [13], [14], [15], [16], [17].

In recent years, higher-order tunable BPFs have been reported. In [18], a 4th-order tunable BPF is presented by employing nonuniform Q -distribution on the dual-mode resonator, which results in a wider 3-dB bandwidth and relatively higher insertion loss. Likewise, 4th-order combline tunable BPFs are presented in [19], [20], and [21] that use microstrip line resonators and varactors. However, the design method of these works is complicated. In [22], 4th-order tunable BPF is designed using three quarter-wave ($\lambda/4$) resonators and one half-wavelength ($\lambda/2$) resonator. A 4th-order

The associate editor coordinating the review of this manuscript and approving it for publication was Feng Lin.

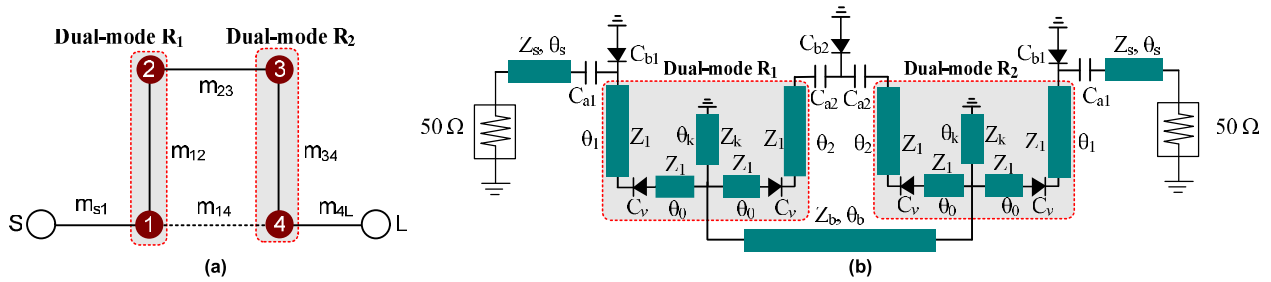


FIGURE 1. (a) Coupling diagram of 4th-order tunable BPF with transmission zeros and (b) circuit implementation of 4th-order tunable BPF using two synchronously tuned dual-mode resonators.

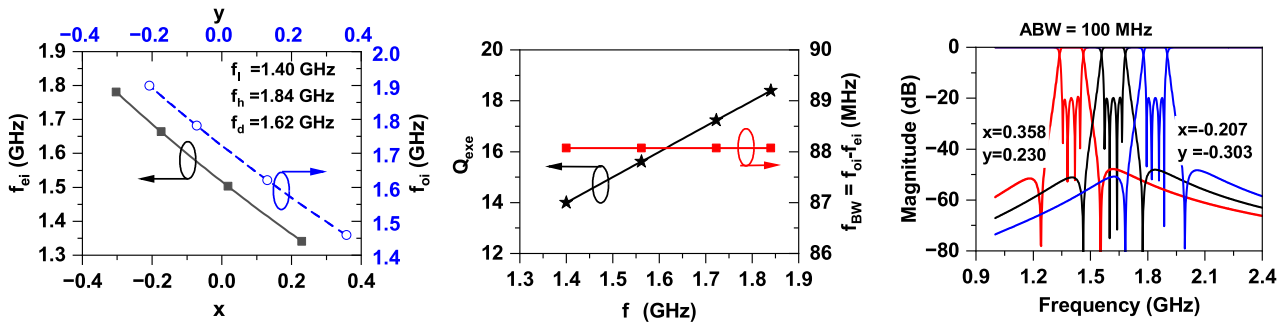


FIGURE 2. Theoretical design parameters and tunable frequency response of 4th-order BPF with constant absolute bandwidth and identical passband response. Coupling matrix values : $m_{s1} = m_{4L} = 1.021$, $m_{12} = m_{34} = 0.8807$, $m_{23} = 0.711$, $m_{14} = -0.06$. Constant ABW = 100 MHz.

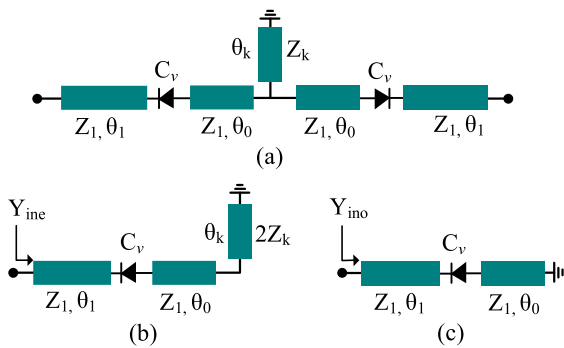


FIGURE 3. (a) Proposed dual-mode resonator, (b) even-mode equivalent circuit and (c) odd-mode equivalent circuit.

tunable BPF with constant ABW is presented in [23] which employs folded topology and cross-coupling between the electric and magnetic coupling resonators. In [24] and [25], a synthesis of higher-order tunable BPF with constant ABW is presented using element-variable coupling matrix (EVCN). For experimental demonstration, 4th-order tunable BPF with constant ABW is fabricated and measured using quarter-wavelength tunable resonators.

More recently, 6th-order tunable BPFs with constant ABW have also been presented. In [26], a 6th-order tunable BPF with constant ABW is presented by using a coupling matrix and frequency-curve shape design approach. Likewise, a 6th-order wideband tunable BPF with constant ABW is demonstrated in [27] using varactor-loaded $\lambda/2$ resonators

and alternate J/K inverters. However, a drawback of these previously reported higher-order tunable BPFs is that passband frequency response is not maintained as the passband frequency is tuned. The passband return loss (RL) is typically degraded while tuning the passband center frequency of the tunable BPFs. In contrast with a lower-order tunable BPF, the higher-order tunable BPFs have more stringent requirements for frequency-dependent coupling while tuning tuning passband frequency. Therefore, designing higher-order tunable BPF with identical passband and constant ABW is quite challenging.

In this paper, we demonstrate a systematic design method for quasi-elliptic higher-order tunable BPFs that consists of synchronously tuned dual-mode resonators, and can achieve identical passband frequency response and constant ABW. To achieve identical passband frequency response and constant ABW, design variables have been extracted such that these design variables can be physically realized easily. The effectiveness of the proposed design method is demonstrated by fabricating 4th- and 6th-order tunable BPFs having passband center frequency tunable from 1.40 GHz to 1.84 GHz and transmission zeros (TZs) at lower and upper sides of passband.

II. DESIGN THEORY

A. 4th-ORDER TUNABLE BPF WITH CONSTANT ABSOLUTE BANDWIDTH

Fig. 1(a) shows coupling diagram of 4th-order tunable BPF with TZs. The TZs at lower and upper sides of passband are

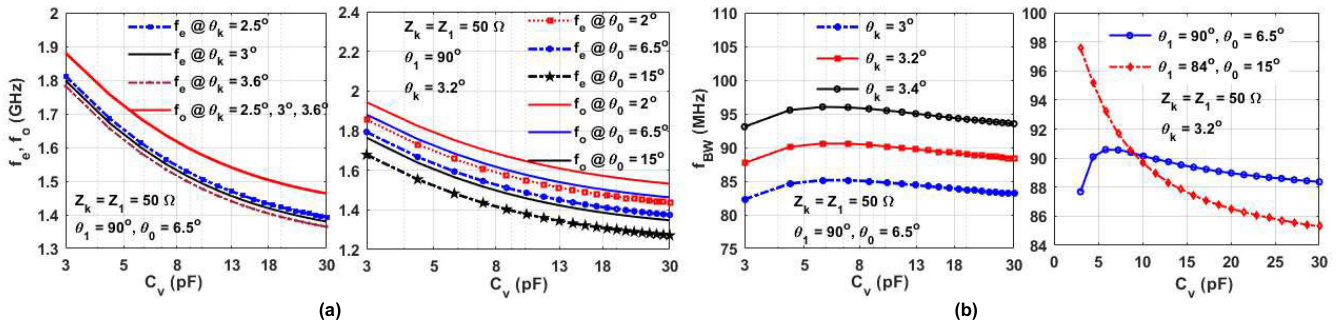


FIGURE 4. (a) Even and odd-mode resonant frequencies (f_e and f_o) and (b) bandwidth $f_{BW} = (f_o - f_e)$ responses with different θ_1 , θ_0 , and θ_k . Electrical lengths are defined at 1.50 GHz.

generated by cross-coupling between resonators. To reduce the number of resonators, Fig. 1(b) shows circuit implementation of 4th-order tunable BPF, where resonators 1 and 2 as well as resonators 3 and 4 are implemented using two synchronously tuned dual-mode resonators R_1 and R_2 . The even and odd-mode resonant frequencies of dual-mode resonator play an important role for achieving constant ABW in the proposed tunable BPF. The self-coupling element value of dual-mode resonators can be written as (1) in terms of even- and odd-mode resonant frequencies (f_{ei} and f_{oi}) of dual-mode resonators.

$$x = \left(\frac{f_d}{f_{ei}} - \frac{f_{ei}}{f_d} \right), y = \left(\frac{f_d}{f_{oi}} - \frac{f_{oi}}{f_d} \right), i = 1, 2, \dots \quad (1)$$

where mapping frequency element f_d is given as $f_d = (f_h + f_l)/2$ and f_h and f_l are upper and lower limits of tunable center frequency of filter. As seen from (1), self-coupling coefficients are dependent on f_d , which leads to design tunable BPF.

To design the tunable BPF with constant ABW and identical passband frequency response, the separation between odd- and even-mode resonant frequencies (f_{ei} and f_{oi}) should be constant desired value ($ie f_{BW} \cong f_{oi} - f_{ei}$). To achieve constant ABW, even and odd-mode resonant frequencies of dual-resonators should be determined using (2) where f_c is a tunable passband center frequency of BPF between f_h and f_l .

$$f_{ei} = f_c - ABW \times m_{i,i+1}, i = 1, 3, \dots \quad (2a)$$

$$f_{oi} = f_c + ABW \times m_{i,i+1}, i = 1, 3, \dots, \quad (2b)$$

where $m_{i,i+1}$ is a coupling matrix value as shown in Fig. 1(a). Once even and odd-mode resonant frequencies are determined, coupling between dual-mode resonators ($k_{i,i+1}$), and external Q -factor (Q_{exe}) should be determined using (3).

$$k_{i,i+1} = \frac{ABW}{f_c} \times m_{i,i+1}, i = 2, 4, \dots \quad (3a)$$

$$Q_{exe} = \frac{Q_e + Q_o}{2} = \frac{f_{e1} + f_{o1}}{2 \times ABW} \quad (3b)$$

Using (1)-(3), theoretical calculated design parameters and frequency response of tunable filter are shown in Fig. 2. As seen from the figure, even-mode resonant frequencies move from 1.359 GHz to 1.80 GHz when x is tuned

from 0.358 to -0.207 and odd-mode resonant frequencies move from 1.44 GHz to 1.881 GHz when y is tuned from 0.23 to -0.303. Likewise, when center frequency varies from 1.40 GHz to 1.84 GHz, the Q_{exe} is in range of 14 to 18.4. To demonstrate the tunable filter design, center frequency tuning behaviors of BPF are performed by changing x and y and results are extracted. As depicted in Fig. 2, the passband center frequency of BPF is tuned from 1.40 GHz to 1.84 GHz with constant 1-dB ABW of 110 MHz when x ranges from 0.358 to -0.207 and y ranges from 0.23 to -0.303.

1) RESONANT FREQUENCY OF PROPOSED DUAL-MODE RESONATOR

Fig. 3(a) shows the proposed structure of transmission line (TL) dual-mode resonator which consists of two TLs with characteristic impedance and electrical lengths of Z_1 , θ_0 , θ_1 , varactor diode with a capacitance of C_v , and shunt short-circuited TL with characteristic impedance and electrical length of Z_k , and θ_k . Using the even- and odd-mode equivalent circuits shown in Fig. 3(b) and 3(c), the even- and odd-mode input admittances are derived using (4).

$$Y_{ine} = j \frac{1}{Z_1} \left\{ \frac{Z_L^e \tan \theta_1 - Z_1}{Z_L^e + Z_1 \tan \theta_1} \right\} \quad (4a)$$

$$Y_{ino} = \frac{j}{Z_1} \left\{ \frac{\omega Z_1 C_v (\tan \theta_0 \tan \theta_1 - 1) - \tan \theta_1}{\omega Z_1 C_v (\tan \theta_0 + \tan \theta_1) - 1} \right\}, \quad (4b)$$

where

$$Z_L^e = \frac{2Z_1 Z_k \tan \theta_k + Z_1^2 \tan \theta_0}{Z_1 - 2Z_k \tan \theta_k \tan \theta_0} - \frac{1}{\omega C_v} \quad (5)$$

The even- and odd-mode resonant frequencies (f_e and f_o) can be extracted by equating $im(Y_{ine}) = 0$ and $im(Y_{ino}) = 0$. The center frequency and BW are predefined as $f_c = (f_e + f_o)/2$ and $f_{BW} = (f_o - f_e)$, and corresponding response analysis is carried out by changing θ_1 , θ_0 , θ_k , and capacitance of varactor model 1T362 varactor from Sony Inc with $C_v = 3 \sim 30$ pF.

Fig. 4(a) shows the even and odd-mode resonant frequencies with different θ_0 and θ_k . The even-mode resonant frequency moves close to the odd-mode as θ_k decreases. Similarly, even and odd-mode resonant frequencies advances

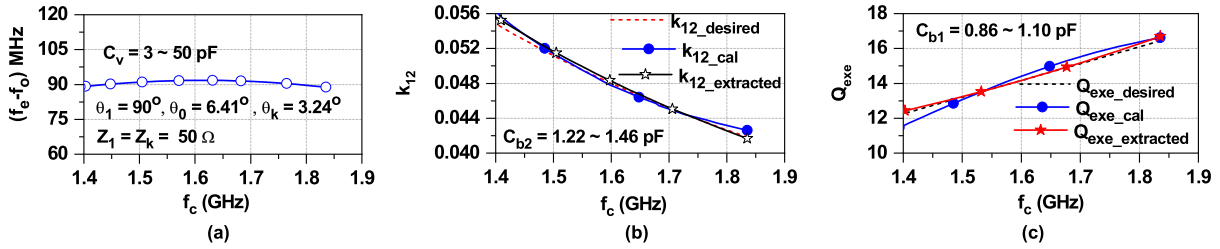


FIGURE 5. (a) Even- and odd-mode resonant frequencies separation, (b) coupling coefficient between dual-mode resonators, and (c) external quality factor. C_v is varied from 3 ~ 50 pF with values of $Z_1 = Z_s = Z_k = 50 \Omega$, $\theta_1 = 90^\circ$, $\theta_2 = 80^\circ$, $\theta_0 = 6.41^\circ$, $\theta_k = 3.24^\circ$, $\theta_s = 52.9^\circ$, $C_{a1} = 0.7$ pF, and $C_{a2} = 0.5$ pF. Electrical lengths of transmission lines are defined at 1.50 GHz.

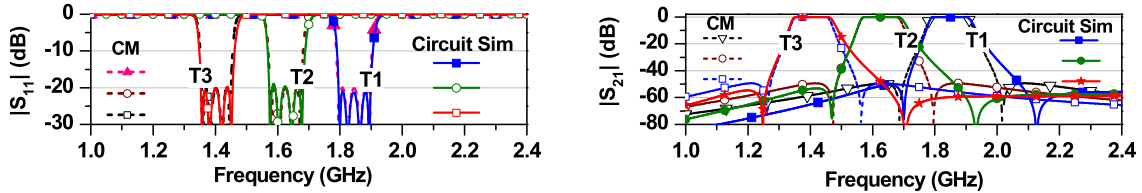


FIGURE 6. Simulation results of 4th-order tunable BPF. Dashed line: coupling matrix results and solid line : circuit simulated results. Circuit parameters: $Z_s = Z_1 = Z_k = 50 \Omega$, $\theta_1 = 52.9^\circ$, $\theta_2 = 79.2^\circ$, 78.8° , $\theta_0 = 6.41^\circ$, $\theta_k = 3.24^\circ$, $\theta_s = 52.9^\circ$, $C_{a1} = 0.7$ pF, $C_{a2} = 0.5$ pF, $Z_b = 60 \Omega$, $\theta_b = 20^\circ$.

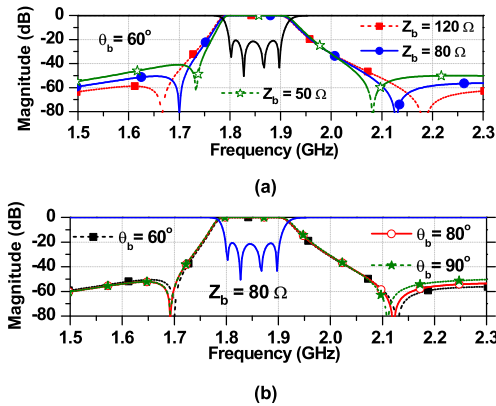


FIGURE 7. Simulation results of 4th-order BPF with controlling TZs according to (a) Z_b and (b) θ_b .

toward higher frequency as θ_0 decreases. Fig. 4(b) depicts the f_{BW} according to θ_1 , θ_0 , and θ_k . The constant f_{BW} can be achieved by adjusting θ_k . Likewise decreasing f_{BW} is obtained when θ_0 is slightly larger such as 15° . Based on these analysis, tunable BPF with different absolute bandwidth can be realized easily using the proposed dual-mode resonator.

2) INTER-RESONATOR AND INPUT/OUTPUT PORT COUPLING

The inter-resonator coupling between dual-mode resonators is implemented through series capacitors C_{a2} and shunt varactor capacitance C_{b2} . The series capacitors C_{a2} will also act as DC-block capacitor between dual-mode resonators. The addition of C_{a2} and C_{b2} will shift resonant frequency of dual-mode resonators which should be compensated by decreasing electrical length θ_2 of dual-mode resonators.

Similarly, the coupling between dual-mode resonator and input/output RF ports is implemented through series TLs (Z_s, θ_s), fixed series capacitor C_{a1} , and shunt varactor diode capacitance C_{b1} . The series C_{a1} also functions as dc-block capacitor. Addition of C_{a1} will decrease resonant frequencies of dual-mode resonator, which can be compensated by decreasing electrical length θ_1 .

Fig. 1(b) shows overall circuit implementation of the proposed 4th-order tunable BPF. To achieve tunable frequency response with constant ABW, the desired $(f_o - f_e)$ is obtained by properly selecting Z_k and θ_k as shown in Fig. 5(a). Likewise, the desired frequency-dependent coupling coefficient (k_{12}) is obtained by selecting $C_{a2} = 0.5$ pF and varying C_{b2} from 1.22 pF to 1.46 pF as shown in Fig. 5(b). Finally, the desired frequency-dependent external Q -factor is achieved when $C_{a1} = 0.7$ pF and C_{b1} is varied from 0.86 pF to 1.10 pF as shown in Fig. 5(c). The TZs are generated due to the cross-coupling between dual-mode resonators, which is implemented with TL (Z_b, θ_b) as shown in Fig. 1(b).

Fig. 6 shows circuit simulation results of 4th-order tunable BPF with constant ABW of 100 MHz. As observed in the figure, the circuit simulation results are well agreed with coupling matrix (CM) results. To investigate the effects of Z_b and θ_b in TZs, Fig. 7 shows the simulation results. The TZ locations are moved close to the passband when Z_b decreases. However, the TZ locations remained almost same as θ_b varies within $60^\circ \sim 90^\circ$.

B. EXTENSION TO 6th-ORDER TUNABLE BPF

The proposed design procedure can be extended to 6th-order tunable BPF. Fig. 8(a) shows the coupling routing diagram of 6th-order tunable BPF with TZ. To reduce the number of resonators, Fig. 8(b) shows circuit implementation of 6th-order

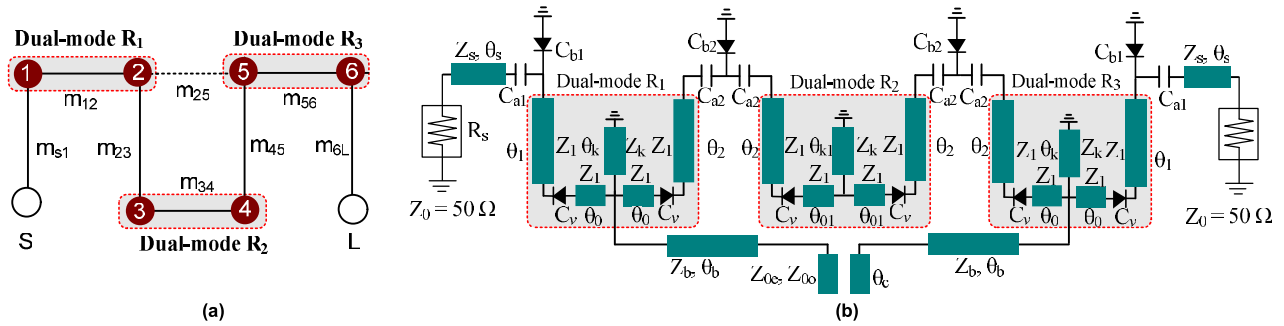


FIGURE 8. (a) Coupling diagram of 6th-order tunable BPF, and (b) microstrip line implementation of 6th-order tunable BPF using three dual-mode resonators.

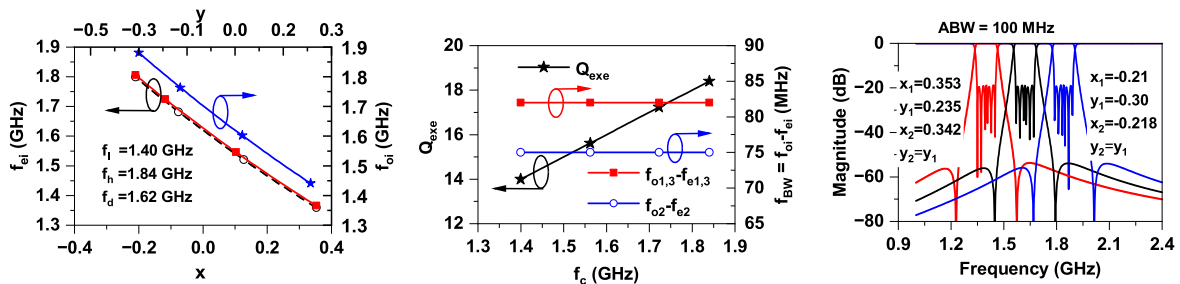


FIGURE 9. Theoretical design parameters and frequency response of the proposed 6th-order tunable BPF using three dual-mode resonators. Coupling matrix : $m_{s1} = m_{6L} = 0.9970$, $m_{12} = m_{56} = 0.8334$, $m_{23} = m_{45} = 0.5911$, $m_{34} = 0.6701$, $m_{25} = 0.1110$. Constant ABW = 100 MHz.

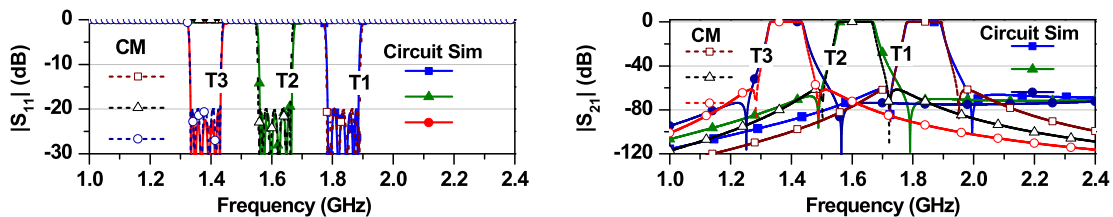


FIGURE 10. Simulation results of 6th-order BPF with constant absolute bandwidth of 100 MHz. Circuit parameters: $Z_s = Z_1 = Z_k = 50 \Omega$, $\theta_1 = 51.6^\circ$, $\theta_2 = 78.8^\circ$, $\theta_0 = 7.24^\circ$, $\theta_{01} = 8.20^\circ$, $\theta_k = 2.95^\circ$, $\theta_{k1} = 2.24^\circ$, $\theta_s = 51.6^\circ$, $C_{a1} = 0.7$ pF, $C_{a2} = 0.5$ pF, $Z_b = 60 \Omega$, $\theta_b = 20^\circ$, $\theta_c = 10^\circ$, $Z_{0e} = 150 \Omega$, $Z_{0o} = 60 \Omega$.

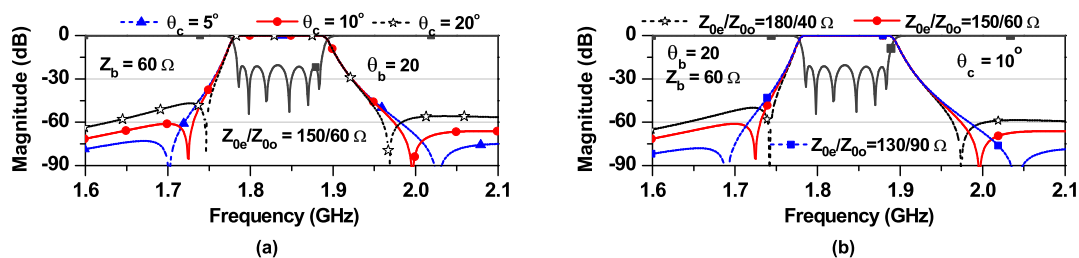


FIGURE 11. Simulation results of 6th-order BPF with controlling TZ according: (a) θ_c and (b) Z_{0e}/Z_{0o} .

tunable BPF where resonators 1 and 2, resonator 3 and 4, and resonator 5 and 6, are implemented using three dual-mode resonators R_1 , R_2 and R_3 . Fig. 9 shows the theoretical design parameters and frequency response of the proposed 6th-order dual-mode tunable BPF with constant ABW of 100 MHz. As seen from the figure, even-mode resonant frequencies

varied from 1.35 to 1.79 GHz when x is tuned from 0.353 to -0.210 whereas odd-mode resonant frequencies varied from 1.441 to 1.88 GHz when y is tuned from 0.235 to -0.30. In order to achieve constant ABW, the separation between odd- and even-mode resonant frequency is 82 MHz for the first and third dual-mode resonator whereas 75 MHz for

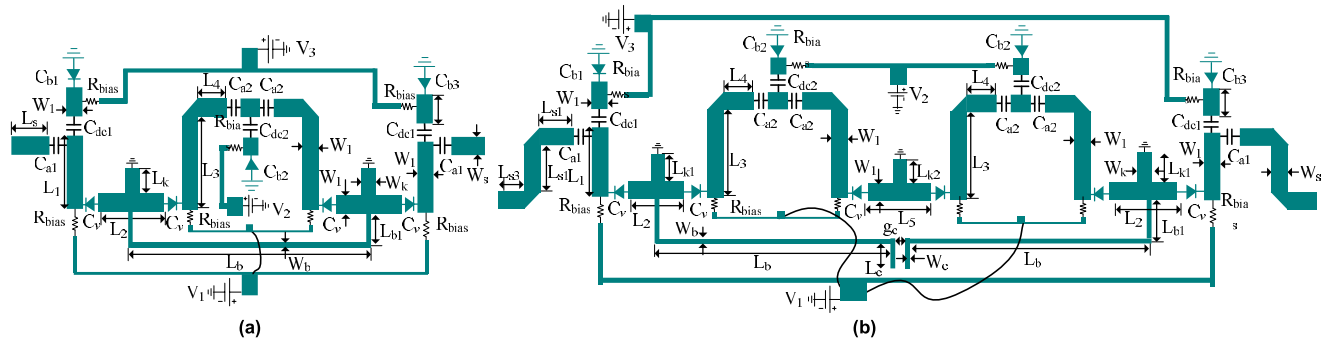


FIGURE 12. (a) Physical layout of 4th-order BPF with dimensions: $W_s = W_L = 1.80$, $W_1 = W_k = 1.38$, $L_s = L_L = 21.5$, $L_1 = 18.5$, $L_2 = 7.48$, $L_3 = 22$, $L_4 = 7.60$, $L_k = 1.90$, $W_b = 0.3$, $L_b = 32.04$, $L_{b1} = 3.80$, $C_{a1} = 0.75$ pF, $C_{dc1} = 0.7$ pF, $C_{dc2} = 0.5$ pF, $C_{a2} = 0.46$ and $R_{bias} = 5$ k Ω and (b) physical layout of 6th-order BPF with dimensions: $W_s = 1.50$, $W_1 = W_k = 1.38$, $L_{s1} = 5$, $L_{s2} = 11$, $L_{s3} = 4.35$, $L_1 = 18.26$, $L_2 = 4.58$, $L_3 = 29$, $L_4 = 1$, $L_5 = 5.5$, $L_{k1} = 2$, $L_{k2} = 1.60$, $L_{b1} = 1.70$, $L_b = 15.195$, $W_b = W_c = 0.6$, $L_c = 1.10$, $g_c = 0.61$, $C_{a1} = C_{a3} = 0.75$ pF, $C_{dc1} =$ pF, $C_{dc2} = 0.9$ pF, $C_{a23} = C_{a45} = 0.46$ pF, and $R_{bias} = 5$ k Ω . C_v , C_{b1} , and C_{b2} : 1T362 from Sony Corporation. Physical dimension unit: millimeter (mm).

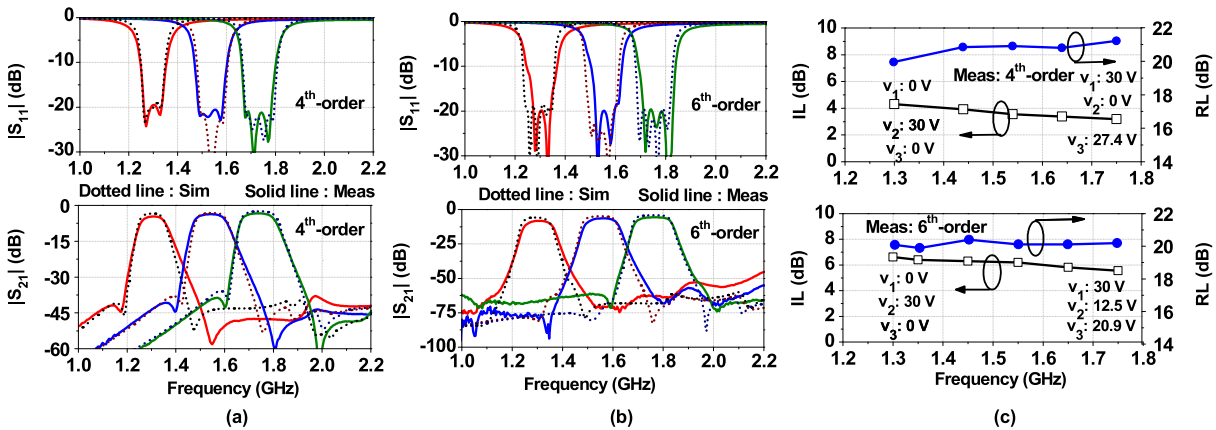


FIGURE 13. Simulation and measurement results with identical passband RL: (a) 4th-order and (b) 6th-order BPF and (c) insertion loss and return loss.

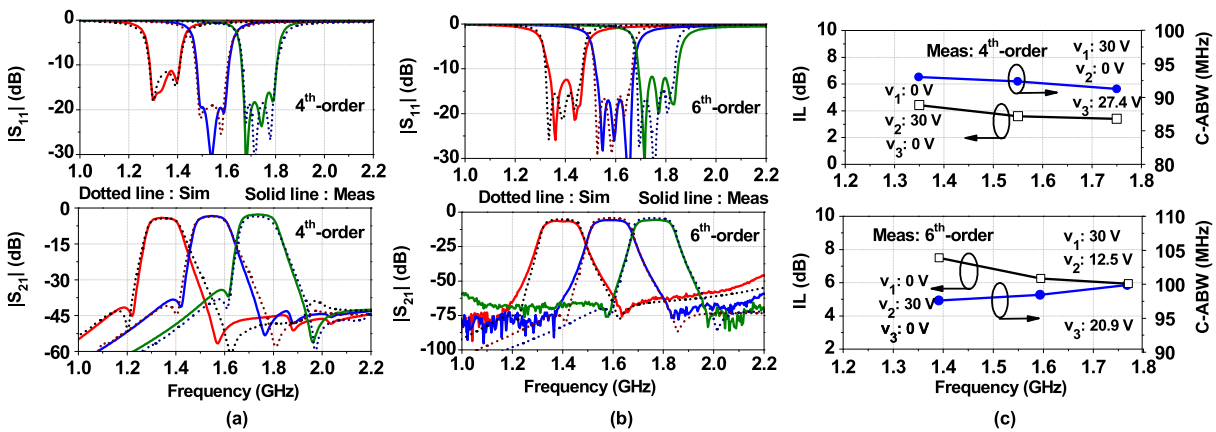


FIGURE 14. Simulation and measured results of tunable BPF with constant absolute bandwidth: (a) 4th-order BPF, (b) 6th-order BPF, and (c) insertion loss and constant absolute bandwidth.

second dual-mode resonator. The external Q -factor varies from 14 to 18.5 when the center frequency is tuned from 1.40 to 1.84 GHz.

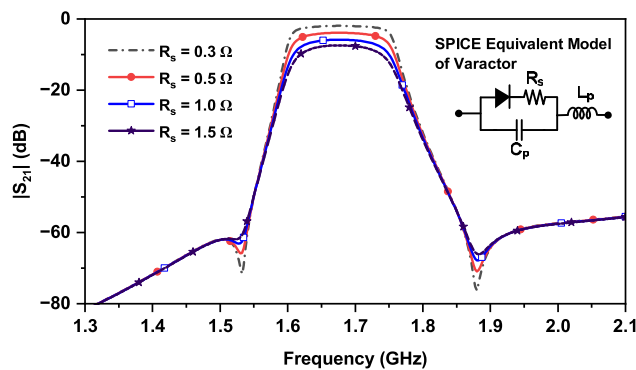
Fig. 10 shows circuit simulation results of microstrip line 6th-order tunable BPF with constant ABW of 100 MHz.

The circuit simulation results are compared with theoretical frequency response obtained through CM. The circuit simulated results are well agreed with CM results. Likewise, the passband RL of 20 dB and the 1-dB constant ABW of 104 ± 1.6 MHz are maintained while tuning the center

TABLE 1. Performance comparison between this work and previously reported frequency-adaptive BPFs.

	Frequency tuning range: FTR (GHz)	IL (dB)	1-dB BW (MHz)	Filter order	Number of varactors	Number of bias voltages	IIP3 (dBm)
[20]	1.55 ~ 2.10 (30.13%)	< 6	80±10*	4 th	10	5	5.5 ~ 17
[21]	1.25 ~ 2.10 (50.74%)	< 8.5	54~162*	4 th	10	5	13 ~ 19
[22]	0.97 ~ 1.53 (44.80%)	< 4.2	54~84*	4 th	6	1	8 ~ 30.3
[23]	0.95 ~ 1.48 (43.60%)	< 4.4	117±3	4 th	6	2	22.9 ~ 34.9
[24]	1.24 ~ 1.72 (32.40%)	< 5.4	94.5±2.5	4 th	4	2	12 ~ 21
[25]	1.05 ~ 1.40 (28.50%)	< 3.5	134±1.5	4 th	4	2	16.3 ~ 29.95
[26]	0.88 ~ 1.12 (24.01%)	< 7.1	40.8±2.4	6 th	6	1	NA
[27]	1.90 ~ 2.30 (19.50%)	< 3.20	580±10*	6 th	6	1	NA
This work	1.35 ~ 1.75 (25.82%)	< 4.40	92±1.30	4 th	7	3	27.2 ~ 39.1
	1.38 ~ 1.77 (24.76%)	< 7.30	98±1.50	6 th	10	3	24.4 ~ 36.1

* : 3dB-bandwidth

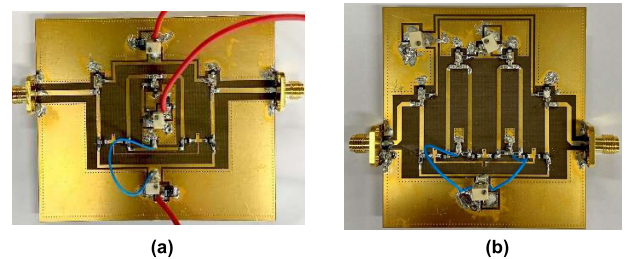
**FIGURE 15.** Simulation results of 6th-order tunable BPF with different parasitic resistance R_s of varactor diode. Other parasitic parameters of varactor : $C_p = 0.31$ pF and $L_s = 2$ nH [28].

frequency from 1.84 GHz to 1.40 GHz. The high frequency selectivity, as well as large attenuation level at stopband are achieved due to higher filter-order and TZs. Fig. 11 shows the simulation results of microstrip line 6th-order tunable BPFs with different TZs locations according to θ_c , Z_{0e} , and Z_{0o} . The TZ locations are moved closer to the passband as θ_c increases. Similarly, TZs locations are moved away from the passband when Z_{0e} decreases and Z_{0o} increases.

III. EXPERIMENTAL RESULTS

For experimental demonstration, 4th and 6th-order tunable BPFs with passband RL of 20 dB and constant ABW of 106 MHz were designed and fabricated. The tunable BPFs are designed using Taconic substrate with a dielectric constant of 2.2, thickness of 0.78 mm, and loss tangent of 0.0009. In this work, varactor diode 1T362 from Sony Corporation is used, which provides diode capacitance of 2.90 pF to 100 pF by varying reverse bias voltage from 30 to 0 V [28]. The series resistance of the varactor diode varies from 0.28 to 0.65 Ω . Fig. 12 shows the layouts of 4th and 6th-order BPF including physical dimensions.

Fig. 13 shows the simulation and measurement results of 4th and 6th-order BPFs. In measurement, the passband center frequency of 4th-order BPF is tuned from 1.30 GHz to 1.75 GHz with passband RL of 20 dB at each of the frequency tuning states. The frequency selectivity is improved due to

**FIGURE 16.** Photograph of fabricated filters : (a) 4th-order and (b) 6th-order tunable BPF.

two TZs at the stopband. The measured insertion loss (IL) varies from 3.18 dB to 4.48 dB. Likewise, the center frequency of 6th-order BPF is tuned from 1.30 GHz to 1.76 GHz with passband RL of 20 dB at each of the frequency tuning states. The attenuation level in the stopband is higher than 50 dB. The measured IL varies from 5.55 dB to 7.90 dB.

Fig. 14 (a) shows the simulated and measurement S -parameter results of 4th-order tunable BPFs with constant ABW. Although finite number of measurement results are shown in Fig. 14(a), it is possible to continuously tune passband center frequency from 1.35 GHz to 1.75 GHz where the return losses are better than 11.8 dB for all frequency tuning states. Likewise, Fig. 14(b) shows simulated and measurement S -parameter results of 6th-order tunable BPF with constant ABW. As seen from measured results, the passband center frequency is tuned from 1.38 GHz to 1.77 GHz. The return losses are better than 11.97 dB for all frequency tuning states.

Fig. 14 (c) shows the measured 1-dB constant ABWs and ILs of 4th-order and 6th-order tunable BPFs according to dc-bias voltage of varactor diodes. From the experimental results, the measured 1-dB constant ABW and IL of 4th-order BPF are determined as 92 ± 1.30 MHz and 3.40 ~ 4.40 dB when passband center frequency is tuned from 1.35 GHz to 1.75 GHz. Similarly, the measured 1-dB constant ABW of 6th-order BPF is 98 ± 1.5 MHz with IL variation of 5.60 dB to 7.30 dB and the passband center frequency variation of 1.38 GHz to 1.77 GHz.

Fig. 16 shows the photograph of fabricated BPFs. The input third-order intercept point (IIP3) was measured with two-tone

input signals separated by 1 MHz. The measured IIP3 varied from 24.4 dBm to 36.1 dBm.

To investigate the cause of high IL, we have performed simulation of 6th-order tunable BPF using SPICE model of varactor diode 1T362 from Sony Corporation and results are shown in Fig. 15. The IL is mainly due to parasitic resistance R_s of varactor diode. As the value of R_s increases, the IL also increases. The IL can be improved relatively if varactor diode with low parasitic resistance (high Q-factor varactor diode) is used.

Table 1 compares the performances of the proposed tunable BPF against the previously reported counterparts. The majority of previously reported tunable BPFs are 4th-order except [26], [27]. In [26], a 6th-order BPF with constant ABW is demonstrated, however, frequency tunability range (FTR) is only 240 MHz (0.88 ~ 1.12 GHz). Likewise in [27], 6th-order tunable BPF with constant ABW is demonstrated with FTR of 19.50%, however, constant ABW is wide (such as 580 ± 10 MHz). This work, in contrast, demonstrates 4th- and 6th order BPFs that exhibit 400 MHz (25.82%) FTR with identical passband frequency response and constant ABW depending on designer's requirement.

IV. CONCLUSION

This paper demonstrated a design of higher-order tunable BPFs using synchronously tuned dual-mode resonators that provides identical passband frequency response or constant ABW, which increases design flexibility depending on the designer's requirements. For achieving constant ABW, the frequency-dependent coupling coefficient and external quality factor have been investigated. For proof of concept, the 4th- and 6th-order tunable BPFs were designed, fabricated, and measured. In the physical realization, the selection of coupling regions demonstrated with simple structure, as a result, the fabricated higher-order BPFs results exhibit excellent agreement with theoretical ones. Quasi-elliptic passband response with TZs is obtained while tuning center frequency. In addition, the proposed design method can easily extend to higher-order filter such as 8th-order tunable BPF with constant ABW.

REFERENCES

- [1] R. J. Cameron, R. Mansour, and C. M. Kudsia, *Microwave Filters for Communication Systems: Fundamentals, Design and Applications*. Hoboken, NJ, USA: Wiley, 2007.
- [2] W. Tang and J.-S. Hong, "Varactor-tuned dual-mode bandpass filters," *IEEE Trans. Microw. Theory Techn.*, vol. 58, no. 8, pp. 2213–2219, Aug. 2010.
- [3] H.-J. Tsai, N.-W. Chen, and S.-K. Jeng, "Center frequency and bandwidth controllable microstrip bandpass filter design using loop-shaped dual-mode resonator," *IEEE Trans. Microw. Theory Techn.*, vol. 61, no. 10, pp. 3590–3600, Oct. 2013.
- [4] L. Athukorala and D. Budimir, "Compact second-order highly linear varactor-tuned dual-mode filters with constant bandwidth," *IEEE Trans. Microw. Theory Techn.*, vol. 59, no. 9, pp. 2214–2220, Sep. 2011.
- [5] D. Lu, N. S. Barker, and X. Tang, "A simple frequency-agile bandpass filter with predefined bandwidth and stopband using synchronously tuned dual-mode resonator," *IEEE Microw. Wireless Compon. Lett.*, vol. 27, no. 11, pp. 983–985, Nov. 2017.
- [6] D. Lu, X. Tang, N. S. Barker, M. Li, and T. Yan, "Synthesis-applied highly selective tunable dual-mode BPF with element-variable coupling matrix," *IEEE Trans. Microw. Theory Techn.*, vol. 66, no. 4, pp. 1804–1816, Apr. 2018.
- [7] D. Lu, X. Tang, N. S. Barker, and Y. Feng, "Single-band and switchable dual-/single-band tunable BPFs with predefined tuning range, bandwidth, and selectivity," *IEEE Trans. Microw. Theory Techn.*, vol. 66, no. 3, pp. 1215–1227, Mar. 2018.
- [8] J.-R. Mao, W.-W. Choi, K.-W. Tam, W. Q. Che, and Q. Xue, "Tunable bandpass filter design based on external quality factor tuning and multiple mode resonators for wideband applications," *IEEE Trans. Microw. Theory Techn.*, vol. 61, no. 7, pp. 2574–2584, Jul. 2013.
- [9] Z. Zhao, J. Chen, L. Yang, and K. Chen, "Three-pole tunable filters with constant bandwidth using mixed combline and split-ring resonators," *IEEE Microw. Wireless Compon. Lett.*, vol. 24, no. 10, pp. 671–673, Oct. 2014.
- [10] P.-L. Chi, T. Yang, and T.-Y. Tsai, "A fully tunable two-pole bandpass filter," *IEEE Microw. Wireless Compon. Lett.*, vol. 25, no. 5, pp. 292–294, May 2015.
- [11] C. Ge and X.-W. Zhu, "Highly-selective tunable bandpass filter with two-path mixed coupling," *IEEE Microw. Wireless Compon. Lett.*, vol. 24, no. 7, pp. 451–453, Jul. 2014.
- [12] G. Basavarajappa and R. R. Mansour, "Design methodology of a tunable waveguide filter with a constant absolute bandwidth using a single tuning element," *IEEE Trans. Microw. Theory Techn.*, vol. 66, no. 12, pp. 5632–5639, Dec. 2018.
- [13] Y.-C. Chiou and G. M. Rebeiz, "A tunable three-pole 1.5–2.2-GHz bandpass filter with bandwidth and transmission zero control," *IEEE Trans. Microw. Theory Techn.*, vol. 59, no. 11, pp. 2872–2878, Nov. 2011.
- [14] Y.-C. Chiou and G. M. Rebeiz, "A quasi elliptic function 1.75–2.25 GHz 3-pole bandpass filter with bandwidth control," *IEEE Trans. Microw. Theory Techn.*, vol. 60, no. 2, pp. 244–249, Feb. 2012.
- [15] B.-W. Kim and S.-W. Yun, "Varactor-tuned combline bandpass filter using step-impedance microstrip lines," *IEEE Trans. Microw. Theory Techn.*, vol. 52, no. 4, pp. 1279–1283, Apr. 2004.
- [16] A. J. Alazemi and G. M. Rebeiz, "A low-loss 1.4–2.1 GHz compact tunable three-pole filter with improved stopband rejection using RF-MEMS capacitors," in *IEEE MTT-S Int. Microw. Symp. Dig.*, May 2016, pp. 1–4.
- [17] T. Yang and G. M. Rebeiz, "A simple and effective method for 1.9–3.4-GHz tunable diplexer with compact size and constant fractional bandwidth," *IEEE Trans. Microw. Theory Techn.*, vol. 64, no. 2, pp. 436–449, Feb. 2016.
- [18] H. Guo, J. Ni, and J. Hong, "Varactor-tuned dual-mode bandpass filter with nonuniform Q-distribution," *IEEE Microw. Compon. Lett.*, vol. 28, no. 11, pp. 1002–1004, Nov. 2018.
- [19] H.-M. Lee and G. M. Rebeiz, "A 640–1030 MHz four-pole tunable filter with improved stopband rejection and controllable bandwidth and transmission zeros," in *IEEE MTT-S Int. Microw. Symp. Dig.*, Jun. 2013, pp. 1–3.
- [20] Y. C. Chiou and G. M. Rebeiz, "Tunable 1.55–2.1 GHz 4-pole elliptic bandpass filter with bandwidth control and >50 dB rejection for wireless systems," *IEEE Trans. Microw. Theory Techn.*, vol. 61, no. 1, pp. 117–124, Jan. 2013.
- [21] T. Yang and G. M. Rebeiz, "Tunable 1.25–2.1-GHz 4-pole bandpass filter with intrinsic transmission zero tuning," *IEEE Trans. Microw. Theory Techn.*, vol. 63, no. 5, pp. 1569–1578, May 2015.
- [22] L. Gao and G. M. Rebeiz, "A 0.97–1.53-GHz tunable four-pole bandpass filter with four transmission zeroes," *IEEE Microw. Wireless Compon. Lett.*, vol. 29, no. 3, pp. 195–197, Mar. 2019.
- [23] D. Tian, Q. Feng, and Q. Xiang, "Synthesis applied 4th-order constant absolute bandwidth frequency-agile bandpass filter with cross-coupling," *IEEE Access*, vol. 6, pp. 72287–72294, 2018.
- [24] D. Lu, X. Tang, M. Li, and N. S. Barker, "Four-pole frequency agile bandpass filter with fully canonical response and constant ABW," in *IEEE MTT-S Int. Microw. Symp. Dig.*, May 2018, pp. 1–3.
- [25] D. Lu, M. Yu, N. S. Barker, Z. Li, W. Li, and X. Tang, "Advanced synthesis of wide-tuning-range frequency-adaptive bandpass filter with constant absolute bandwidth," *IEEE Trans. Microw. Theory Techn.*, vol. 67, no. 11, pp. 4362–4375, Nov. 2019.
- [26] M. Ohira, S. Hashimoto, Z. Ma, and X. Wang, "Coupling-matrix-based systematic design of single-DC-bias-controlled microstrip higher order tunable bandpass filters with constant absolute bandwidth and transmission zeros," *IEEE Trans. Microw. Theory Techn.*, vol. 67, no. 1, pp. 118–128, Jan. 2019.

- [27] X.-G. Huang, J.-Q. Zhang, Y.-Q. Lin, and Q.-Y. Xiang, "Design of a six-pole tunable band-pass filter with constant absolute bandwidth," in *Proc. Prog. Electromagn. Res. Symp. (PIERS)*, 2016, pp. 3507–3510.
- [28] *IT362: Silicon Variable Capacitance Diode*, Sony Corporation, New York, NY, USA, pp. 1–4.



GIRDHARI CHAUDHARY (Member, IEEE) received the B.E. degree in electronics and communication engineering from the Nepal Engineering College (NEC), Kathmandu, Nepal, in 2004, the M.Tech. degree in electronics and communication engineering from MNIT, Jaipur, India, in 2007, and the Ph.D. degree in electronics engineering from Jeonbuk National University, Republic of Korea, in 2013.

He is currently working as a Contract Professor with the JIANT-IT Human Resource Development Center, Jeonbuk National University. Previously, he was a Principal Investigator on an independent project through the Basic Science Research Program administrated by the National Research Foundation (NRF) and funded by the Ministry of Education. His current research interests include multi-band tunable passive circuits, magnetless non-reciprocal circuits, in-band full duplex systems and high-efficiency power amplifiers, and the applications of negative group delay circuits. He was a recipient of the BK21 PLUS Research Excellence Award from the Korean Ministry of Education, in 2015. He was also a recipient of the Korean Research Fellowship (KRF) through the NRF funded by the Ministry of Science and ICT.



YONGCHAE JEONG (Senior Member, IEEE) received the B.S.E.E., M.S.E.E., and Ph.D. degrees in electronics engineering from Sogang University, Seoul, Republic of Korea, in 1989, 1991, and 1996, respectively.

From 1991 to 1998, he was a Senior Engineer with Samsung Electronics, Seoul. Since 1998, he has been with the Division of Electronics Engineering, Jeonbuk National University, Jeonju, Republic of Korea. From July 2006 to December 2007, he was a Visiting Professor with the Georgia Institute of Technology. He was the Director of the HOPE-IT Human Resource Development Center, BK21 PLUS, and the Vice-President of planning with Jeonbuk National University. He is currently a Professor with Jeonbuk National University. He has authored and co-authored more than 260 papers in international journals and conference proceedings. His current research interests include active and passive microwave circuits for mobile and satellite base-station RF systems, periodic defected transmission lines, negative group delay circuits and their applications, in-band full duplex radio, and RFIC design. He is a member of the Korea Institute of Electromagnetic Engineering and Science (KIEES).

...